Thermodynamic assessment of RuO4 oxide

Ioana Nuta, François Virot, Evelyne Fischer, Christian Chatillon

Thermodynamic assessment of RuO_4 oxide

Ioana Nuta*[1], Francois Virot[2], Evelyne Fischer[1] and Christian Chatillon[1]

[1] Univ. Grenoble Alpes, CNRS, Grenoble INP, SIMaP, F-38000 Grenoble, France
1130 rue de la piscine BP 75 38402 Saint Martin d'Hères
[2] Institut de Radioprotection et de Sûreté Nucléaire (IRSN, PSN-RES/SAM), 13115 Saint Paul Lez Durance, France

* Corresponding author: Ioana Nuta, Tel: +33 476826511;
E-mail address: ioana.nuta@ grenoble-inp.fr

Abstract

RuO_4 oxide appears much less stable than RuO_2(s) in the Ru-O binary system with a melting point close to room temperature and a certain propensity to vaporize or decompose at low temperatures. Ab initio simulations in the framework of density functional theory (DFT) on RuO_4(s) are performed to analyze the cubic and monoclinic structures and to evaluate the heat capacities at low temperatures. Then, a critical evaluation of thermodynamic data from calorimetry and vapor pressure determinations - was carried out coupled with ab-initio calculations to propose new thermodynamic data: the entropy,
$S°$ (RuO_4, s, cubic, 298K) = 132.7 $J{\cdot}K^{-1}mol^{-1}$ and formation enthalpy,
$\Delta_f H°$ (RuO_4, s, cubic, 298K) = -252.4 ± 5.5 kJ mol^{-1}.

Keywords: RuO_4, Ru-O, Entropy, Formation enthalpy

Introduction

In the event of a hypothetical severe accident in a nuclear power plant, the potential release of highly radiotoxic fission products (FPs), such as ruthenium, is of particular concern [1-6].
RuO_4(g) shows a high volatility at low temperatures and many groups suspect that it is the source of ruthenium transport in a carrier gas flowing over organic or aqueous solutions used in nuclear effluent treatment. [6-13]. In previous studies - (i) we proposed new thermodynamic data for RuO_2 (s) [14] *i.e.* heat capacity, entropy and enthalpy of formation, - (ii) we revised the standard formation enthalpies as well as the entropies of RuO_4(g), RuO_3(g), RuO_2(g) and RuO(g) [15] and compared them with calculations from the SSUB database[16] and with the ab-initio data given by Miradji [17]. The low temperature region of the Ru-O phase diagram is not accurate and some data are missing. The compound RuO_4(s) exists in the binary system in oxygen-rich compositions and in the low temperature range since it melts at 298.65 K according to Debray and Joly [18] and at 298.55 K according to Nikol'skii [19]. The enthalpy of formation of this compound was determined by calorimetry by Nikol'skii and Ryabov [20] and by Mercer and Farrar [21]. The boiling point (1 atm) of RuO_4 (l) was determined by Koda [22] at T_{eb} = 402.75 ± 0.2 K. The vapor pressure in the range 273 to 363 K - probably in the form of the RuO_4(g) molecule mainly if no decomposition occurs - was studied by Nikol'skii [23]. These data gives access to the enthalpy of formation of the solid or liquid by using the independently determined enthalpy of

formation of the gaseous RuO_4(g) molecule from a thermodynamic cycle, as already done by Cordfunke and Konings [24].
Despite the important applications of the molecular crystal ruthenium tetroxide compound as an organic oxidant [25] as well as its interest in the field of nuclear safety, some of its properties remain uncertain or are no longer reported in literature. There are currently no experimental data concerning the specific heat at low and high temperatures for the compound RuO_4 (s, or liq).
Using original data we recalculate the thermodynamic functions to improve the description proposed in the last compilation performed in 1990 by Cordfunke and Konings [24].

1 Results and discussions

1.1 Thermal functions

There is no experimental data for the low and high temperature heat capacities. In Appendix A we present our method for DFT calculations performed to obtain the heat capacity $C°_p$ at low temperature, and the deduced entropy and Gibbs energy function (free energy function referred to 0 K) for the RuO_4(s, cubic) crystal. Hence, we propose the following relation,

$$C_p^\circ(RuO_4(s, cubic, T) = -53.426 - 0.32993T + \frac{127.66}{T} + 17.071\sqrt{T}$$

reliable in the 10 – 298.6K range. The entropy value calculated by integration of C°p as 132.7 J K^{-1} mol^{-1} is compared with those proposed in literature (see Appendix I, Table A-2). Acceptable agreement is obtained with data extracted from the online database [26] while those published in the 1990s are excluded [24].
In the absence of low temperature specific heat $C°_p$ experimental data, the entropy could be also estimated by Latimer's rule [27-29] from the ionic contributions to entropy at 298 K for oxides and compounds (see Appendix B). The so-estimated entropy which is 132.5 J K^{-1} mol^{-1} it is in agreement with the DFT based value.

Finally, the entropy retained in this work is,

$$S^\circ\ (RuO_4, s, cubic, 298K) = 132.7\ J\ K^{-1} mol^{-1}.$$

For the liquid phase, after melting at 298.6K, the heat capacity is considered to be constant and equal to the value of the solid at melting (298.6K), *i.e.* $C°_p$ = 91.598 J K^{-1} $mol^{-1,}$ a value given by the least squares adjustments as proposed in Appendix I.

Enthalpy and entropy of melting are discussed in more detail with the vapor pressure data from Nikol'skii [23]. Free energy function for the condensed phases, calculated in this way,

$$Fef^\circ\ (RuO_4, s\ or\ liq, 298K) = S_T^\circ - \frac{H_T^\circ - H_{298}^\circ}{T}$$

is presented in figure 1.

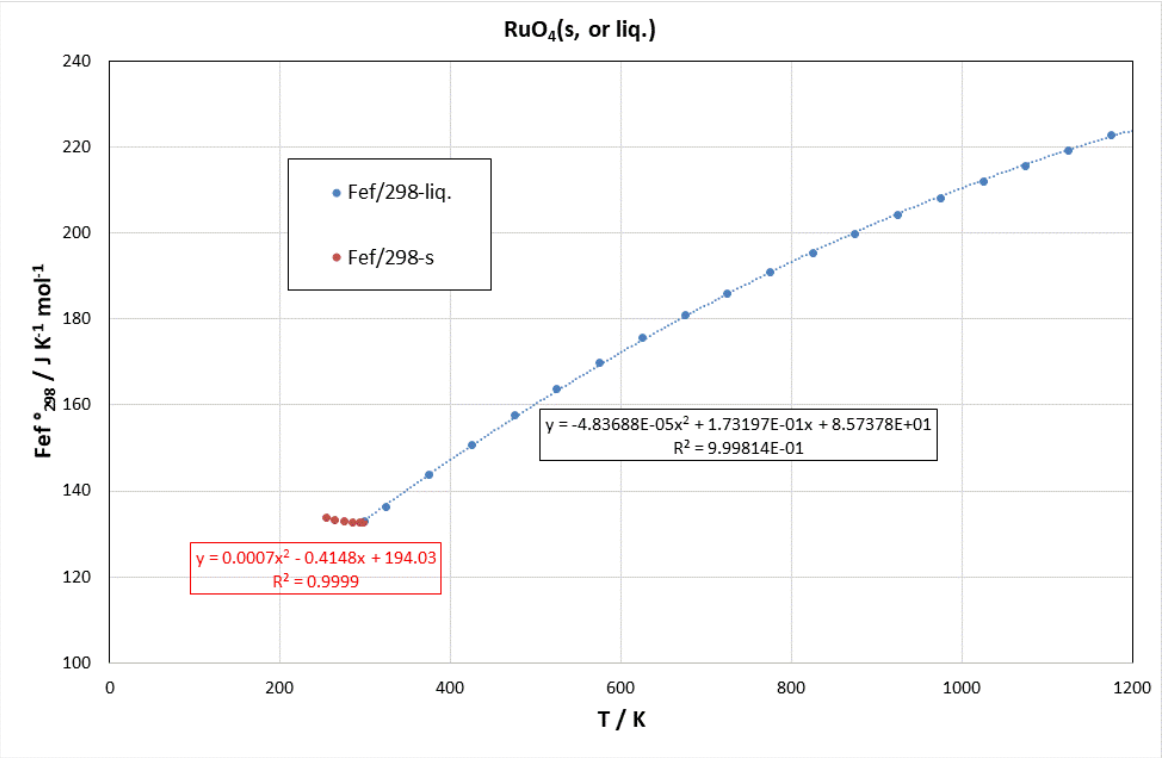

Figure 1. Gibbs (or free) energy function referred to 298 K for RuO_4 (s) and RuO_4 (liq) calculated from solid and liquid heat capacities, entropy at 298 K and enthalpy of fusion.

1.2 Enthalpy of formation

1.2.1 Bomb calorimetry

As in this work we recalculate all intermediate relations, the presentation will be in kcal (1 cal = 4.184 J) to allow the reader to compare with the original Russian publication (reference [19]). Table 1 also reproduces directly the original publication. Final results are presented in kJ.

In 1964, Nikol'skii and Ryabov [20] prepared RuO_4 (s) by transport and condensation in a glass ampoule stored at liquid nitrogen temperature. The ampoule is introduced into a calorimeter filled with NH_3 at high pressure. The reaction between RuO_4 (s, or l) and the NH_3 gas was studied in a calorimetric bomb under 10 and 5 atm of NH_3 and for temperatures close to the melting of the oxide. Two simultaneous reactions are assumed to occur,

$$3\ RuO_4\,(s, or\ liq.) + 4\ NH_3\,(g) = 3\ RuO_2\,(s) + 6\ H_2\,O\,(l) + 2\ N_2\,(g) \qquad \boldsymbol{Q_2\ (R2)}$$

$$3\ RuO_4\,(s, or\ liq.) + 8\ NH_3\,(g) = 3\ Ru\,(s) + 12\ H_2\,O\,(l) + 4\ N_2\,(g)\,. \qquad \boldsymbol{Q_3}\ ^{1}\boldsymbol{(R3)}$$

These reactions were confirmed by XRD and chemical analysis of the solid residue. The authors [20] did not detect any NO_x molecules in the produced gas phase meanwhile they did not mention their analytical tool. The proportions of solids for each reaction - expressed as

[1] *N.B. Quantities* $\boldsymbol{Q_2}$ *and* $\boldsymbol{Q_3}$ *quoted here are the heats received by the calorimeter.*

mole fraction "a" - are determined by analysis of the residue after each combustion experiment. The reactions are carried out either with RuO_4 (l) at 26°C or with RuO_4 (s) at 24°C – the temperature of the bomb calorimeter. In parallel, water as a reaction product reacts with ammonia - this could be a dissolution forming a solution of NH_3 in water. Previously, the authors determined the heat of reaction between water and ammonia at 10 atm (proposed as 8.53 ± 0.1 kcal mol^{-1}) and 5 atm (4.65 ± 0.1 kcal mol^{-1}). Note that the above reactions assume that there is no dissolution of solids in water, particularly for RuO_4 whose solubility in water is discussed below.

The authors [20] combine reactions ***(R2)*** and ***(R3)*** to derive the value of the difference $\boldsymbol{Q_3 - Q_2}$ mentioned in their relation *(4)*, that corresponds to the reaction

$$3\ RuO_2\ (s) + 4\ NH_3\ (g) = 3\ Ru\ (s) + 6\ H_2O\ (l) + 2\ N_2\ (g).\quad \boldsymbol{Q_3 - Q_2}$$

with a heat balance calculated from the standard enthalpies of the compounds as proposed,

$$\boldsymbol{Q_3 - Q_2} = -\ (\Delta H°_3 - \Delta H°_2) = 147.4\ \text{kcal}.$$

This relationship allows the calculation of the enthalpy $\Delta H°_i$ or the heat determined at constant pressure. As written, the two values $\boldsymbol{Q_3}$ and $\boldsymbol{Q_2}$ are therefore no longer considered as heats that the calorimeter receives at constant volume (or internal energy received by the calorimeter bomb and lost by the system) but as heats at constant pressure (enthalpies). The minus sign in front of the enthalpies confirms that the heats *Q* are those received by the calorimeter[2].

On the basis of n_{init} moles of RuO_4(s, or l) and with a mole fraction "*a*" calculated from the chemical analysis according to reaction ***(R2)*** and *"(1-a)"* to reaction ***(R3)***, the authors expressed the total energy at constant volume released by these two simulated reactions alone, a heat that the calorimeter receives,

$$Q = \frac{n}{3}[a\ (Q_2 - 2\ RT) + (1 - a)(Q_3 - 4\ RT)]\ .$$

The heat of reaction *Q* is in principle the total heat measured by the calorimeter bomb, *i.e.* at constant volume. The heats $\boldsymbol{Q_2}$ and $\boldsymbol{Q_3}$ are heats at constant pressure produced by the two reactions and received by the calorimeter (thermal effect). The RT terms correspond to the work, *i.e.* with *VdP = dn RT*, produced at constant volume in the calorimeter when the number of gaseous moles *dn* created or lost in the two reactions is taken into account and changes the pressure. Finally, the authors propose,

$$Q\ (kcal) = n\ \left(\frac{Q_3}{3} - 48{,}73\ a - 0{,}79\right).$$

The pressure variation in the calorimetric bomb must be taken into account, that makes the calculation of the heat at constant volume difficult and problematic. The main question is how to transform heat at constant pressure, ΔH, into heat at constant volume, ΔU, knowing that

[2] The authors mentioned in their relation ***(4)*** a value of $\boldsymbol{Q_3 - Q_2}$ =147.4 kcal. From the enthalpies mentioned in their paper, we calculate a value of $Q_3 - Q_2$ = -147.36 kcal. The difference in sign clearly confirms that the constant volume heats, Q_2 and Q_3, mentioned by the authors first, are indeed the thermal effects that the calorimeter receives. In contrast, the enthalpies are related to chemical reactions. A value of $\boldsymbol{Q_3 - Q_2}$ = - ($\Delta H°_3$ - $\Delta H°_2$) = 142.265 kcal was recalculated using the enthalpy of formation of RuO_2 (s) that we critically retained in a previous work [14] and the JANAF [30] tables for gaseous ammonia and liquid water.

ΔQ is not a state function while ΔH and ΔU are. According to the fundamental definition of heat (Prigogine [31] p. 24), the enthalpy of reactions ***(R2)*** and ***(R3)*** is expressed as a function of the internal energy E (or U) and the work by this relation :

$$H=U+pV.$$

Using the first principle (Prigogine [31] p. 19) written as

$$dU = dQ – pdV,$$

the differential of H becomes,

$$dH = (dQ - pdV) + Vdp + pdV = dQ + Vdp.$$

Therefore, the heat exchanged by the chemical system at constant volume is related to the enthalpy at constant pressure for any reaction by:

$$dQ = dH - VdP.$$

It is this heat *dQ* supplied by the constant volume system that will be received by the calorimeter for each reaction ***(R2)*** and ***(R3)*** *i.e.* $\boldsymbol{Q_2}$ and $\boldsymbol{Q_3}$ as mentioned in their paper. Calculation of the thermal effect received by the calorimeter must be related to the enthalpies ΔH_2 and ΔH_3 at constant pressure given by the authors or from our original data selection. Relation *(5)* will become:

$$Q = \frac{n}{3}[a\,(\boldsymbol{Q_2}) + (1-a)(\boldsymbol{Q_3})] = \frac{n}{3}[a\,(-(\mathrm{dH} - \mathrm{VdP})_2) + (1-a)(-(\mathrm{dH} - \mathrm{VdP})_3)].$$

Assuming an ideal gas, the term *Vdp* is a function of the number of moles,

$$Vdp = RT\,dn$$

dn being the variation in the number of moles between the two terms of the reaction. For reaction ***(R2)*** *dn = -2*, and for reaction ***(R3)*** *dn = -4*. Indeed, the heats mentioned by Nikol'skii and Ryabov [20] $\boldsymbol{Q_2}$ and $\boldsymbol{Q_3}$ are equal to,

$$\boldsymbol{Q_2} = -(\Delta H°_2 + 2RT)$$

$$\boldsymbol{Q_3} = -(\Delta H°_3 + 4RT)$$

and relation (5) of Nikol'skii and Ryabov [20] becomes,

$$Q = \frac{n}{3}\left[a\left(-\Delta H_2^\circ - 2\,RT\right) + (1-a)(-\Delta H_3^\circ - 4\,RT)\right].$$

This relationship is the one proposed by Nikol'skii and Ryabov [20] with $\boldsymbol{Q_2}$ and $\boldsymbol{Q_3}$ the measured calorimetric values. With our reference for the enthalpy of formation values $\Delta_f H(RuO_2,s)$ = -74.58 kcal [14] and JANAF tables [30] $\Delta_f H(NH_3,g)$ = -10.97 kcal and $\Delta_f H(H_2O,liq)$= -68.315 kcal, the heat becomes

$$Q(kcal) = n\left(\frac{-\Delta H_3^\circ}{3} - 47{,}423a - 0{,}7895\right).$$

The quantity *Q* above corresponds only to the two reactions mentioned (2) and (3) when they are stoichiometric. However, the amount of heat measured must also take into account the mixing reaction between the initial NH_3 phase and the created H_2O phase, an amount that was evaluated by the authors in a preliminary calorimetric experiment.

The thermodynamic calculation at 298.15 K of H_2O (l) in contact with NH_3 (g) gives a constant volume enthalpy of 1.73 kcal per mole of water at 10 bar and 2.67 kcal per mole of water at 5 bar considering an ideal mixture. The higher values measured by Nikol'skii and Ryabov [20] are probably related to the dissolution of NH_3 in liquid water with creation of bonds.
The quantity measured by calorimetry $w\,\Delta r$ is,

$$w\,\Delta r = Q(kcal) + 8.53\,n_{H_2O} \;\; at\ 10\ atm$$

and

$$w\,\Delta r = Q(kcal) + 4.65\,n_{H_2O}\ at\ 5\ atm$$

where n_{H2O} is the number of moles of water produced by reactions ***(R2)*** and ***(R3)***, w =1.635 10^{-2} kcal is the calorimeter constant, Δr is the change in thermometer resistance. The number of moles of water produced by the two reactions is,

$$n_{H_2O} = 2n\,(2-a)$$

and therefore, using our reference enthalpy values,

$$1{,}635\ \cdot\ 10^{-2}\Delta r = n\left(\frac{-\Delta H_3^\circ}{3} - 64{,}483\,a + 33{,}3306\right) at\ 10\ atm.$$

$$1{,}635\ \cdot\ 10^{-2}\,\Delta r = n\left(\frac{-\Delta H_3^\circ}{3} - 56{,}723\,a + 17{,}8105\right)\ at\ 5\ atm.$$

From reaction *(R3)*,

3 RuO_4 (s)+ 8 NH_3 (g) = 3 Ru (s) + 12 H_2 O (l) + 4 N_2 (g) $\Delta H°_3$ ***(3)***

as the authors we deduce the relationship

$$-\Delta_f H_{298}^\circ(RuO_4, l) = 244{,}227 - \frac{Q_3}{3} = 244{,}227 - \frac{-\Delta H_3^\circ}{3}.$$

At 10 atm, using our references, the calculated enthalpies are:

$$\Delta_f H_{298}^\circ(RuO_4, l) = -277{,}558 + \frac{w\Delta r}{n} + 64{,}483a$$

and at 5 atm,

$$\Delta_f H_{298}^\circ(RuO_4, l) = -262{,}838 + \frac{w\Delta r}{n} + 56{,}723a.$$

These last two equations we use with our chosen values for *NH_3 (g).* In the case where *NH_3* is liquid, the relations (4) and *(5)* become

Q_3 **-** ***Q_2*** = - ($\Delta H°_3$ -$\Delta H°_2$) = 109.38 kcal with our references

$$\text{with}\ \ Q = \frac{n}{3}\left[a\left(-\Delta H_2^\circ - 2\,RT\right) + (1-a)(-\Delta H_3^\circ - 4\,RT)\right]$$

then $Q = n\left(-\frac{\Delta H_3^\circ}{3} - 36{,}065\,a - 0.7895\right)$.

Experiments with NH_3 (liq) performed under 10 atm:

$$w\,\Delta r = Q(kcal) + 8{,}53 \cdot 2n\,(2-a)\;for\;10\;atm$$

$$w\,\Delta r = n\left(-\frac{\Delta H_3^\circ}{3} - 53{,}125\,a + 33{,}3306\right).$$

From reaction (***R3***) with NH_3 liquid,

$$\Delta_f H_{298}^\circ(RuO_4, l) = -222{,}086 + \frac{Q_3}{3} = -222{,}086 + \frac{-\Delta H_3^\circ}{3} \quad \text{from our references}$$

By importing the enthalpy values ΔH°_3 of reaction (R3) we obtain the relationship

$$\Delta_f H_{298}^\circ(RuO_4, l) = -255{,}417 + \frac{w\Delta r}{n} + 53{,}125\,a.$$

All parameters of the experiments *w, Δr , n* and *a,* are given by Nikol'skii and Ryabov [20] in their table allowing us to recalculate the enthalpy of formation of RuO_4 (s, or liq, 298K) as presented in table 1. Our re-calculations reproduce those of Nikol'skii and Ryabov [20] and, furthermore, new data are obtained with theses references. The average values calculated for the RuO_4 liquid are,

$$\Delta_f H^\circ(RuO_4\text{ , liq, 298K}) = -\,226.4 \pm 7.5\ \text{kJ mol}^{-1}$$

The uncertainties listed here are standard deviations and they are directly related to the reproducibility of the experiments.

Table 1. Comparison between the Nikol'skii and Ryabov [20] calorimetric data as recalculated from their published relationships and with our new reference values.

Initial mix RuO_4 + NH_3			RuO_2 product	ΔH_f (RuO_4) liq			Rel. (11),(12) *Nikol'skii and Ryabov[20]*	**This work** (11bis) (12a)
Exp. Nb.	conditions	mMol initial	Molar fraction A	Table 1 Nikol'skii and Ryabov	With relationship	Δr in Ω	ΔH_f (RuO_4) liq. or solid /kcal mol^{-1}	ΔH_f (RuO_4) liq. or solid /kcal mol^{-1}
1	10 bar, RuO_4 liq,NH_3 g	1.164	0.58	-52.4	11	13.3	-52.4	**-53.3**
2		2.314	0.748	-55.4	11	24.45	-55.4	**-56.6**
3		1.723	0.473	-52.2	11	20.45	-52.2	**-53.0**
4		1.544	0.335	-53.1	11	19.1	-53.1	**-53.7**
5		1.76	0.651	-55.2	11	19.3	-55.3	**-56.3**
6	5 bar RuO_4 liq, NH_3 g	1.436	0.53	-55.8	12	15.4	-55.7	**-57.4**
7		2.52	0.631	-53.3	12	26.5	-53.3	**-55.1**
8		2.13	0.437	-56.9	12	23.4	-56.9	**-58.4**
9		3.74	0.667	-56.8	12	38.65	-54.2	**-56.0**
10	NH_3 liq + RuO_4 liq	0.749	0.554	-57	13	7.9	-57.0	**-53.5**
11	RuO_4 (s) 10 bar	2.61	0.537	-53.7	11	29.65	-44.7*	**-41.2***
12		2.275	0.348	-57.1	11	27.1	-46.6*	**-42.2***
13	NH_3 liq + RuO_4 liq	3.03	0.676	-55.7	13	30.4	-58.3	**-55.5**

**Nikol'skii and Ryabov[20] are different for the solid because they results included the heat of fusion (from their vapor pressures: see section 1.3).*

The values for solid RuO_4 (s) can be deduced from our analysis (section 1.3.1.) of the vapor pressures measured on RuO_4 ,

$$\text{or } \Delta_f H°(RuO_4\text{ , s, 298K}) = -\ 239.7 \pm 7.5 \text{ kJ mol}^{-1}$$

Nikol'skii and Ryabov[20] take into account of NH_3 dissolution in the created aqueous phase but neglected the RuO_4(s) dissolution studied later by Nikol'skii [22]. This dissolution reaction probably exothermic competes with the combustion for the heat received by the calorimeter. This heat contribution should be deduced from the measured Q value by the calorimeter as done for NH_3 dissolution and same effect is attended: the deduced formation enthalpy would slightly decrease.

1.2.2 Thermal analysis

In 1965 Watt and McMordie [32] observed frank ignition when they mixed NH_3 (g) with RuO_4 (s) at -70°C. To avoid this ignition, they added small increments of NH_3 (g) under 10^{-3} Torr to RuO_4 (s) starting at -70°C. They observed some reactions detected by a black coloration of the solution formed turning brown at -50°C. No reaction products were found by X-ray analysis. Using thermogravimetric analysis (TGA) and a temperature ramp of 3°C/min, an explosion occurred at 206°C. From the infrared absorption analysis, they proposed the formation of the compound $Ru_4N_{11}O_{12}H_{33}$ since similar absorption bands were observed with the compound Os. The authors believe that Nikol'ski and Ryabov [20] actually measured other reactions by calorimetry. However, since Nikol'ski and Ryabov [20] analyzed all their reaction products by XRD and chemical analysis to determine the RuO_2 (s) / Ru(s) ratio, we believe that the bomb calorimetric reactions observed under NH_3(g) high pressure remain very different from those observed by Watt and McMordie. [32] This is probably due to the actual operating temperature range of the bomb as well as the higher pressure of NH_3 .

1.2.3 Dissolution in water Calorimetry

Mercer and Farrar (1969) [21] performed dissolution calorimetry measurements in an aqueous medium. Firstly, the authors carried out a reaction between Br_2 (liq.) and Ru(s) powder dispersed in a solution of NaOH (1 mol l^{-1}): the bromine is enclosed in a bulb that is immersed in soda. After reaching thermal equilibrium in the calorimeter, the ampoule is broken and a thermal effect is recorded. Two main reactions that take place simultaneously are proposed,

$$Ru(s) + 3\ Br_2\ (liq.) + (a\ NaOH, b\ H_2O) = [Na_2RuO_4, 6\ NaBr, (a-8)\ NaOH, (b+4)\ H_2O]\ \Delta H_1$$

$$3\ Br_2\ (liq.) + (a\ NaOH, b\ H_2O) = [5\ NaBr, NaBrO_3, (a-6)\ NaOH, (b+3)\ H_2O]. \quad \Delta H_2$$

The square brackets indicate an aqueous solution. The total heat or enthalpy observed is,

$$\Delta H_{obs.}(mol^{-1}Br_2) = \frac{\Delta H_1}{3} + \frac{f_D}{3}\ (\Delta H_2 - \Delta H_1)$$

relationship where f_D is the fraction of Br_2 entering the two reactions (called disproportion) in relation to the total introduced. This factor is calculated from the analysis of the concentration of RuO_4^{2-} ions formed (analysis of the Na_2RuO_4 content). A linear fit of the observed enthalpy to the factor f_D gives the enthalpies ΔH_1 and ΔH_2. The authors found that the deduced enthalpy ΔH_2 and that proposed in an NBS report agree and this result confirms the two competing reactions cited. Next, three other reactions in solution are used to obtain the

enthalpy of formation of sodium ruthenate Na_2 RuO_4 in the basic solution. Note that two approximations are made in the summation, *i.e.* for the heats of formation of NaBr(aq) and water in the pure state. From the heat of formation of Na^+ (aq) at infinite dilution, the heat of formation of the RuO_4^{2-} *(aq)* ion is -109.4 ± 1.0 kcal mol^{-1} (- 457.7 ± 4.2 kJ mol^{-1}) that the authors estimate to be close to the standard enthalpy of formation.

Nine other dissolution reactions using numerous intermediate compounds ($BaCl_2$, $NaIO_4$, $NaIO_3$) in the acid phase ($HClO_4$) make it possible to precipitate the compound RuO_4 (liq. at 26°C) and to determine its enthalpy of formation from 19 enthalpies: six of these enthalpies of dissolution come from the calorimetric investigations of the authors, the others are known reactions. The final value proposed by the authors is:

$$\Delta_f H°(RuO_4, liq, 299K) = -238.5 \pm 4.6 \text{ kJ mol}^{-1}$$

The uncertainties quoted by the authors largely overlap with those existing for the many intermediate reactions used and quoted. Perhaps the authors take into account their three approximations in the uncertainty domain. The present calorimetric determination overlaps with the determination of Nikol'ski and Ryabov[20] determination within the limits of their overall uncertainties.

Mercer and Farrar [21] quote an enthalpy of formation for the RuO_4^{2-} (aq) ion = -109.4 ± 1.0 kcal mol^{-1} (- 457.7 ± 4.2 kJ mol^{-1}) being more negative than the final product RuO_4 (s. or liq. 299K) proposed by Nikol'skii and Ryabov [20]. However, as RuO_4^{2-} (aq) ion is formed by dissolution of RuO_4 in water, the difference between these two studies in the proposed enthalpy of formation of RuO_4 (s, or l) may arise from the dissolution in this medium that is produced in bomb calorimetry experiments.

1.3 Volatility of RuO_4 (s, or l)

1.3.1 Determination of vapor pressures

Nikol'skii (1963) [23] determined the total saturated vapor pressure using a Bourdon gauge constructed with glass (Pyrex) in the temperature range 22°C to 91°C (295-364K). The Bourdon gauge is immersed in a thermostatically controlled liquid bath regulated at ± 0.02°C. Another series of measurements were carried out in the low temperature range from 0.4 to 50°C by calibrated radiometry by cross-checking with the previous results. The temperature is reported to be known within ± 0.1°C. This work is presented in figure 2.

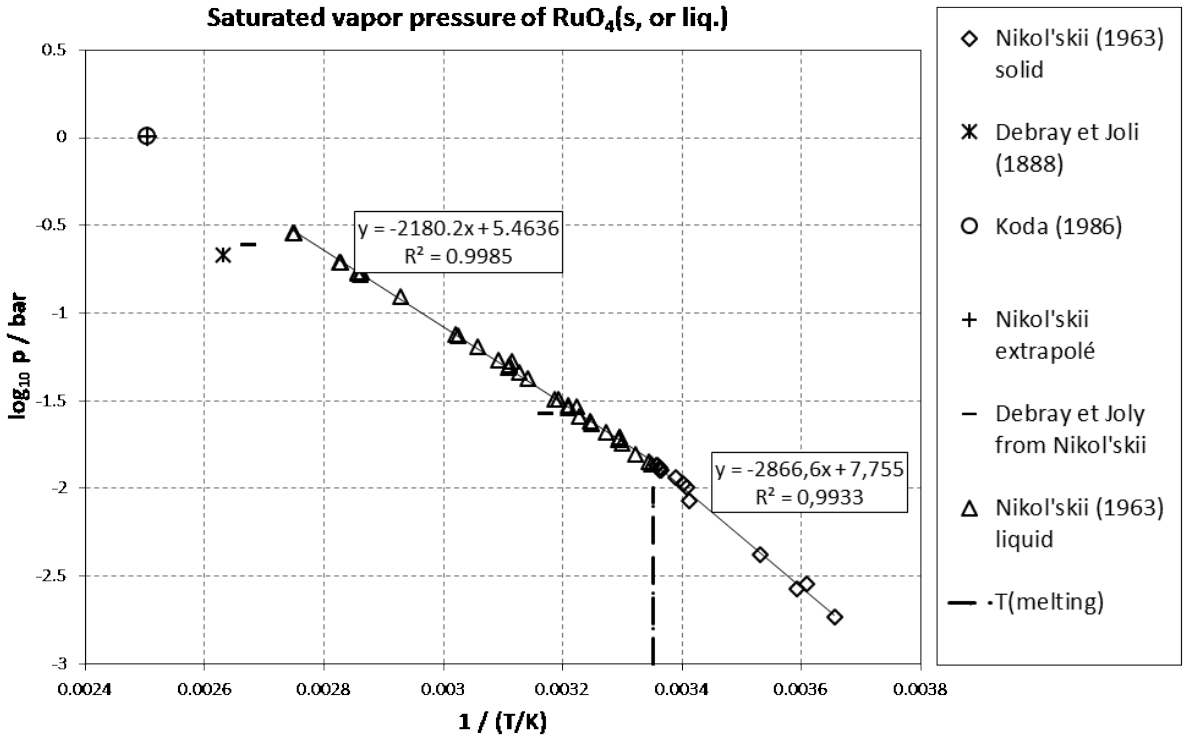

Figure 2 Total vapor pressure as measured on RuO_4 (s, or liq.) according to literature

Koda (1986) [22] more recently determined the boiling point of RuO_4 (l) at 1 atm. This pressure is in agreement with the extrapolated experimental data of Nikol'skii [23]. We also detail very old data from Debray and Joly (1888) [18]. These authors observed a certain instability of the RuO_4 as it easily decomposes into black RuO_2 (s) under atmospheric pressure with probably a release of oxygen. The higher pressure boiling point data from Koda [22] assumes that no decomposition of the oxide occurs in a closed system when atmospheric pressure is not operating.

In Nikol'skii's experiments [23] the preparation of the compound RuO_4 (s) takes place "in situ" by sublimation/condensation of a high-temperature input vapor phase composed mainly of RuO_4(g) and O_2(g) molecules. During the condensation process, oxygen is removed by pumping. Other gaseous oxides such as RuO_3 (g) are probably in very small amounts in the initial vapor phase - see previous analysis by Nuta et al.[15] on the gas phase in the Ru-O binary system - and their condensation in the deposit may form an orange RuO_4 (s) oxide with excess O_2 (g) rather than the RuO_2 (s) - RuO_4 (s) diphase that quickly turns grey or black.

The ionization potentials determined by Dillard and Kiser [33] in the mass spectrometric observation of the vapor phase of RuO_4 (l) introduced directly into an ion source confirm the hypothesis that the RuO_4(g) molecule is major in the saturated vapor phase since they identify only the RuO_4(g) parent molecule by the RuO_4^+ molecular ion and possibly some traces of RuO_3 (g). Thus, the vapor pressure determined by Nikol'skii [23] is rich in RuO_4 (g), although in the RuO_2 (s) - RuO_4 (s, or liq) two-phase domain, there is also an equilibrium pressure of O_2 (g). This could be lower than RuO_4 (g) although higher than that calculated in the Ru(s) - RuO_2 (s) domain $\approx 1.4\ 10^{-44}$ bar at 298 K.

Brittain and Hildenbrand [34] observed the evaporation of RuO_4(s) with a quadrupole mass spectrometer using a two-compartment effusion cell constructed of Pyrex. The lower compartment, loaded with RuO_4(s) and maintained at a temperature between -30 and -78°C, is

connected by a tube and a monel valve to the upper compartment maintained at a temperature between 20 and 130°C. The connection tube is fitted with a Pt baffle at the entrance to the upper cell to impose sufficient collision (and thermal equilibrium) in the upper compartment fitted with the effusion orifice. The lower compartment is kept at a constant temperature throughout the experiment (under high vacuum) to supply the upper compartment with a constant molecular flow or inlet pressure. With the upper compartment at 20°C, the authors first observed the O_2^+ ion (from oxygen) for at least one hour when the connecting valve was opened, and, then, the RuO_4^+ (molecular ion of RuO_4(g)) appeared and remains stable, *i.e.* at constant pressure "although O_2^+ is still present in the vapor (sic)". After experiment, the authors observed a black deposit in the whole effusion device and they propose a first passivation of the wall materials by RuO_2 (s) deposits. These observations mean that the commercial RuO_4(s) material began to decompose during storage (although kept at -5°C) and during introduction of the device into the mass spectrometer. However, the authors point out that the oxygen pressure remains stable when RuO_4 (g) was detected and this means that decomposition occurred in parallel with the production of RuO_4 (g) in the upper cell. In a second specific experiment, the upper compartment was heated up to 130°C while the lower compartment remains at a constant temperature assuming a constant inlet flow and pressure in the upper compartment. Such an experiment therefore allows the decomposition of RuO_4(g) into e.g. RuO_3(g), RuO_2(g), RuO(g), Ru(g) and O_2(g) to be observed. The authors observed a 20% decrease in the intensity of RuO_4^+ and its disappearance at 190°C, whereas the other molecules were not observed. It can be seen that for a constant applied pressure of RuO_4 (g) in the upper compartment, according to the Knudsen relation, the increase in temperature produces a decrease in the Knudsen flow to the mass spectrometer ion source. According to Knudsen's relation,

$$\frac{dN(RuO_4)}{dt} = \frac{\mathrm{p}(RuO_4)sC}{\sqrt{2\pi M_{RuO_4}RT}} \ .$$

with a constant pressure p_{RuO_4} the decrease in relative flow rate (as detected by the ion source) between 20 and 130°C is,

$$d\left[\frac{dN(RuO_4)}{dt}\right] = \frac{\left({}^{1}/_{\sqrt{403}} - {}^{1}/_{\sqrt{293}}\right)}{{}^{1}/_{\sqrt{293}}} \approx 0.15.$$

This value, close to that observed in spectrometry, suggests that RuO_4(g) does not decompose in this temperature range - at least in the sensitivity range of their quadrupole. Indeed, the disappearance of the RuO_4^+ ion at 190°C may also be due to a poor sensitivity of the quadrupole. Note also that the authors encountered significant difficulties in their measurement technique: - (i) black deposits of RuO_2 (s) in the ion source, requiring frequent disassembly and cleaning of the ionization source, - (ii) poor resolution of the true molecular beam with respect to multiple re-evaporations of the volatile RuO_4(g), due to the design of their shuttering device, as evidenced by a residual shuttering effect, as explained in figure 3.

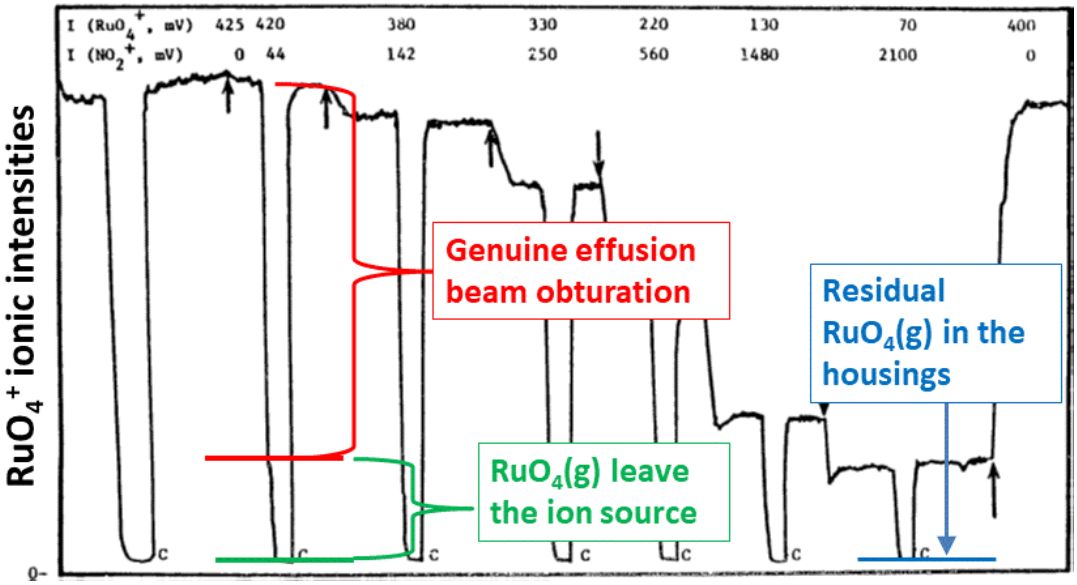

Figure 3. Different ionic intensities of RuO_4^+ observed by Brittain and Hildenbrand [34] in mass spectrometry upon introduction of NO_2 (g) and, then, activation of the molecular beam shutter. First, the introduction of NO_2 (g) into the effusion cell decreases the pressure of RuO_4 (g) at the black arrows (probably the interaction of some decomposition reaction). Then, the shutter movement shows successively a first instantaneous decrease due to the occultation of the real molecular beam coming directly from the effusion orifice (measurement of the real partial pressure of RuO_4 (g)), followed by a re-vaporization of the stable RuO_4 deposits in the ionization box, and, finally, some residual pressure of RuO_4 (g) is detected in the background in relation with the capacity of the pumping device and the ambient temperature.

In conclusion, after an initial heterogeneous reaction between RuO_4(g) and the Pyrex or platinum walls producing a deposit of RuO_2(s), the decomposition of RuO_4 (g) in the gas phase seems to be limited in the temperature range corresponding to the Nikol'skii [23] vapor pressure experiment but the relative proportion between O_2^+ and RuO_4^+ has not been evaluated - and consequently their pressure ratio -. Furthermore and as a confirmation, a low rate of decomposition into RuO_2 (s) + O_2 (g) was measured by Ortner et al (1961) [35] in the range 100 - 160°C. These authors give an Arrhenius law preceded by an incubation time. Finally, a net decomposition occurred above 1025°C, analyzed by Thermogravimetry. These observations confirm that the probable vapor phase is relatively pure RuO_4 (g) in the Nikol'skii experiments but with an unknown proportion of oxygen. This proportion of oxygen may be reduced due to the in-situ elaboration of RuO_4 (s) during pumping and storage at liquid nitrogen temperature, but could increase during the experiment performed in a closed Bourdon gauge.

1.3.2 Standard Enthalpy of melting by second law

The vaporization enthalpy of RuO_4 (s, or liq.) assuming the vapor is composed mainly of RuO_4 (g) species can be calculated by the second and third laws of thermodynamics. The enthalpy of fusion is deduced from the enthalpies of sublimation and vaporization calculated from the slopes (second law) as shown in Figure 2 using Nikol'skii[23] total pressure data for the solid and liquid. The latter set is in agreement with Koda's [22] boiling point that is retained it in this work. The second law calculations give an enthalpy of vaporization for the liquid of 41.74 ± 0.29 kJ mol^{-1}, and for the solid, 54.9 ± 1.3 kJ mol^{-1}, the uncertainties quoted being the standard deviations. The enthalpy and entropy of fusion of RuO_4 at 298.6 K are then deduced:

Δ_{fusion} H°(RuO_4 , s→liq, 298.6K) = 13.3 ± 0.9 kJ mol^{-1}

$$\Delta_{fus}S° = \frac{\Delta_{fus}H°}{T_{fus}} = \frac{13300}{298.6} = 44.541\ J\ K^{-1}mol^{-1}.$$

1.4 Standard Enthalpy of Vaporization

Assuming that the main vaporization reaction of solid or liquid RuO_4 produces the single species RuO_4 (g) in the vapor phase, the free enthalpy of the vaporization reaction of the RuO_4 (s, or liq) is written,

$$\Delta_{vap}G_T^\circ = -RT\ln\frac{P_{RuO_4(g)}}{a_{RuO_4(s,or\ liq)}} = \Delta_{vap}H_T^\circ - T\Delta_{vap}S_T^\circ$$

relation where the activity $a_{RuO_4(s,or\ liq)} = 1$. From this relationship, the standard enthalpy of vaporization at 298.15 K (presently sublimation) can be calculated by applying the third law of thermodynamics,

$$\Delta_{vap}H_{298}^\circ = -RT\ln P_{RuO_4(g)} + T\Delta_{vap}\left[S_{298}^\circ - \frac{H_T^\circ - H_{298}^\circ}{T}\right].$$

The second term, usually called the free energy (or Gibbs) function, is calculated from the entropies of each reactant at 298K and their heat capacities: The function for RuO_4(g) comes from Nuta et al. [15] while the functions for RuO_4(s), RuO_4(liq) and melting come from this work. The treatment by the third law is presented in table 2.

Table 2. Third law sublimation enthalpy of the solid RuO_4 at 298 K and comparison with the results of the 2nd law of Nikol'skii [23] and Koda [22] determination of the total pressure.

T/K	$\log_{10}$ p/bar	RLn p / J K^{-1} mol^{-1}	Δ_{vap} Fef° $_{298}$ / J K^{-1} mol^{-1}	Δ_{subl} H°(298K) / kJ K^{-1} mol^{-1}
273.55	-2.735	-52.363	147.894	54.8
277.05	-2.543	-48.677	148.132	54.5
278.35	-2.572	-49.237	148.217	55.0
283.25	-2.378	-45.528	148.519	55.0
293.15	-2.069	-39.607	149.040	55.3
293.35	-1.995	-38.189	149.049	54.9
294.05	-1.975	-37.814	149.082	55.0
297.35	-1.878	-35.963	149.226	55.1
297.45	-1.893	-36.236	149.230	55.2
297.65	-1.866	-35.732	149.238	55.1
295.11	-1.940	-37.150	149.129	55.0
297.15	-1.897	-36.323	149.217	55.1
297.97	-1.871	-35.814	149.251	55.1
Melt				
298.65	-1.862	-35.651	147.391	54.7
303.15	-1.741	-33.340	146.899	54.6
303.55	-1.711	-32.750	146.856	54.5
307.95	-1.632	-31.243	146.381	54.7
313.15	-1.495	-28.617	145.826	54.6
313.75	-1.489	-28.514	145.763	54.7
318.25	-1.371	-26.251	145.289	54.6
321.15	-1.277	-24.454	144.986	54.4
323.45	-1.270	-24.308	144.747	54.7
299.01	-1.846	-35.334	147.351	54.6
301.05	-1.803	-34.520	147.128	54.7
303.45	-1.711	-32.750	146.867	54.5
303.61	-1.723	-32.981	146.849	54.6
305.61	-1.676	-32.093	146.633	54.6
308.05	-1.615	-30.917	146.370	54.6
309.87	-1.589	-30.429	146.175	54.7
310.23	-1.535	-29.379	146.137	54.5
311.53	-1.539	-29.455	145.998	54.7
311.67	-1.529	-29.266	145.983	54.6
319.85	-1.336	-25.576	145.121	54.6
321.45	-1.294	-24.775	144.955	54.6
321.63	-1.308	-25.041	144.936	54.7
327.15	-1.190	-22.785	144.366	54.7

-To be continued-

T/K	$\log_{10}$ p/bar	RLn p / J K^{-1} mol^{-1}	Δ_{vap} Fef° $_{298}$ / J K^{-1} mol^{-1}	Δ_{subl} H°(298K) / kJ K^{-1} mol^{-1}
330.57	-1.127	-21.572	144.017	54.7
331.05	-1.124	-21.528	143.969	54.8
341.55	-0.908	-17.382	142.916	54.7
349.25	-0.768	-14.699	142.162	54.8
349.65	-0.777	-14.876	142.123	54.9
350.03	-0.773	-14.804	142.086	54.9
350.19	-0.766	-14.673	142.071	54.9
353.65	-0.713	-13.651	141.737	55.0
353.91	-0.708	-13.560	141.712	55.0
363.59	-0.545	-10.426	140.795	55.0
363.95	-0.546	-10.457	140.761	55.0
Boiling point of Koda				
399.45	0.005823753	0.048	137.590	54.9
			3rd average value law	54.8
			Standard deviation	0.2
			2nd solid law**	54.9
			Standard deviation	1.3
			2nd liquid law**	41.6*
			Standard deviation	0.1

**If the enthalpy of fusion is added, the result is 54.9 kJ mol^{-1}, corresponding exactly to the solid.*

*** Corrections for average temperatures are not applied as these temperatures are close to 298.15K.*

The present 3rd law results lead to the standard enthalpy of formation for RuO_4 (s) at 298 K derived from Nuta et al. [15] selected enthalpy of formation of RuO_4 (g),
i.e. -197.6 ± 5.5 kJ mol.$^{-1}$

$$\Delta_f H°(RuO_4, s, 298K) = -252.4 \pm 5.5 \text{ kJ mol}^{-1}$$

The third law values are practically constant as a function of the measurement temperature (see table 2) and are in agreement with those obtained by the second law. This means that the entropy proposed for RuO_4(s) as well as that calculated for the liquid do not introduce any bias in the calculations of the third law. Moreover, the assumption of the main vapor RuO_4(g) in the Nikol'skii [23] experiments seems reliable.

1.5 Enthalpies of formation of RuO_4(s, or liq.)

The enthalpies of formation analyzed in this work are summarized in table 3, compared with previous compilations. Also included are the solid and gaseous species that were used as references in the thermodynamic cycles leading to the standard enthalpy of formation of RuO_4 (s, or liq.).

Table 3. Comparison of different published standard enthalpies of formation at 298 K with our present results.

Compound or molecules	$\Delta_f H°(RuO_x$, s/g, 298K)- *Standard enthalpy of formation at 298 K*		
	Cordfunke and Könings compilation [24]. / kJ mol^{-1}	Calorimetry Experiences / kJ mol^{-1}	This work / kJ mol^{-1}
RuO_2 (s)	-314.2 ± 0.5	-305. 1	-312.3 ± 1.6 of [14] as a reference
RuO_4 (g)	-188.0 ± 4.0		-197.6 ± 5.5 from [15]
RuO_4 (s)	-243 ± 7	-241 ± 5.4 [20]	-239.7 ± 7.5 from [20]* -252.4 ± 5.5 of [23] with RuO_4(g) vapor -358.1 of [23] with O_2(g) vapor assumption -251.0 ± 5.5 from DFT (see Appendix)
RuO_4 (l)		-238.5 ± 4.6 [21]	- 226.4 ± 7.5 of [20]*

**Note that these values should decrease due the dissolution of RuO_4(s) in the produced water phase that is not entered in the combustion process.*

The thermodynamic cycle using vapor pressure gives an enthalpy value that does not match the calorimetric results. As the calculation of the third law is based on the main gas species RuO_4(g) in equilibrium with the RuO_4 (s, or liq), this assumption may be wrong. Following the various studies on the decomposition of this oxide - either in storage or during transport in the gas phase under vacuum (cf. Brittain and Hildenbrand [34]) - the gas phase on RuO_4 (s,

or liq) could be a mixture RuO_4 (g) + O_2 (g). Thus, another hypothesis may be that a vapor richer in oxygen than RuO_4 (g) and the decomposition occurs according to the main reaction,

$$RuO_4\ (s) = RuO_2\ (s) + O_2\ (g).$$

If the pressure on RuO_4(s, or l) determined by Nikol'skii [23] using a closed Bourdon gauge is mainly composed of oxygen, the equilibrium constant of this reaction at 298.6 K - the melting point of RuO_4 (s) - leads directly to the standard enthalpy of formation of RuO_4(s) using the known enthalpy of RuO_2 (s)[14]:

$$-RT \ln p_{O_2} = \Delta_r H^\circ - T\Delta_r S^\circ$$
$$= \Delta_r H^\circ - T[S°(O_2, 298) + S°(RuO_2, 298) - S°(RuO_4, 298)]$$

$$\Delta_r H^\circ(298) = -RT \ln p_{O_2} + 298 * [S°(O_2, 298) + S°(RuO_2, 298) - S°(RuO_4, 298)]$$

and with a total pressure (assumed = $p(O_2)$, at 293K (20°C) according to Nikol'skii [23]
p = 0.0106 bar,

$$\Delta_r H^\circ(298) = 293\ (-R \ln(0.0106) + [205.147 + 46.15 - 132.7]) = 45824\ (\text{J mol}^{-1})$$

$$\Delta_f H^\circ(RuO_4, 298K) = \Delta_f H^\circ(RuO_2, 298K) - \Delta_r H^\circ(298K) = -312.3 - 45.8$$
$$= -358.1\ kJ\ mol^{-1}$$

The enthalpy of formation of RuO_4 (s) would be -358.1 kJ mol^{-1}, a value far away from the proposed calorimetric values or those deduced from thermodynamic cycles based on RuO_4(g).

The Gibbs energies of mixing - calculated for RuO_4(s) with the current ab-initio entropy - are shown in figure 4, highlighting the instability of the RuO_4(s) compound because it is located above the RuO_2 (s) - ½ O_2 (g) line, except for the calculation based on the assumption of lone oxygen in the vapor phase that is located along the line and thus RuO_4 (s) would be an ideal solution between RuO_2(s) and oxygen. Higher values would explain its propensity to decompose during storage or temperature rises into RuO_2 (s) deposits and oxygen release.

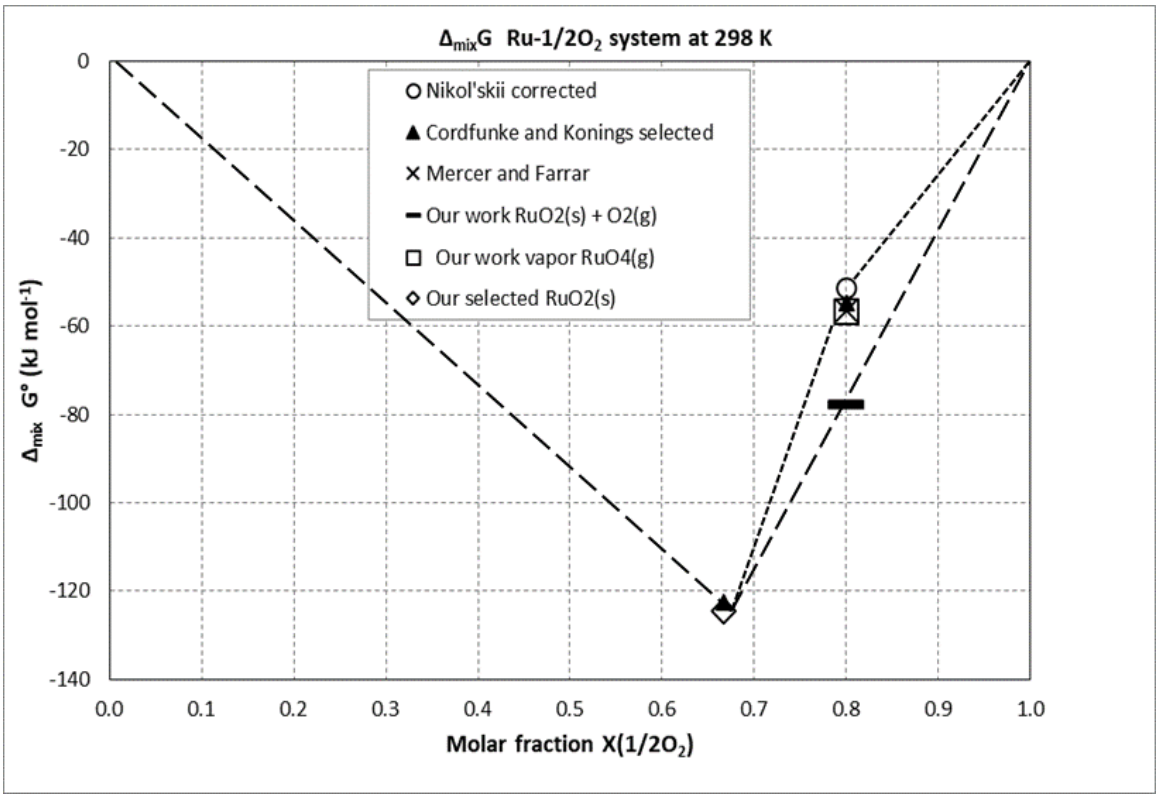

Figure 4. Gibbs's energies of mixing of compounds in the Ru-1/2 O_2 binary system.

To check the consistency of the deduced values, we calculated the equilibrium pressures of oxygen existing on the two-phase mixture RuO_4 (s) - RuO_2 (s) *via the* equilibrium constant of the reaction,

$$RuO_4\ (s) = RuO_2\ (s) + O_2\ (g)$$

corresponding to the release of oxygen with the black RuO_2 (s) deposit as observed by many researchers.

$$-RT \ln p_{O_2} = \Delta_r G^{\circ}_{298} = \Delta_f G^{\circ}_{298}(RuO_2, s) + \Delta_f G^{\circ}_{298}(O_2, g) - \Delta_f G^{\circ}_{298}(RuO_4, s)$$

The equilibrium oxygen pressure calculated with the current free enthalpy values is presented in table 4. With the enthalpy deduced from the vapor pressure of oxygen alone in the Nikol'skii experiments, we obviously find the original pressure introduced in the calculations. For other enthalpy values, the oxygen pressures being very high, this is a good indicator of the instability of the RuO_4(s or liq.) compound compared with RuO_2(s). Thus, it would explain that some experimenters in the past had explosions during temperature increase ramps. This also justifies that the RuO_4(s, or g) is able to release oxygen during storage with low decomposition kinetics as studied for example by Ortner et al. [36]and by Mun et al.[37].

Table 4. Oxygen pressure calculated on the two-phase RuO_4 (s) + RuO_2 (s) at 298K from different proposed formation enthalpies of RuO_4(s). All other thermodynamic functions for RuO_2(s) and RuO_4(s) are those used in this work.

RuO_4 (s) = RuO_2 (s) + O_2 (g)			
Δ_{form} H°(298K) reference for RuO4(s)	Δ_r G °(298K) / kJ mol^{-1}	ln p(O_2)/bar	p(O_2) / bar
Nikol'ski calorimetry [20] corrected (this work)	-103.236	30.810	$2.40 \cdot 10^{13}$
Cordfunke and Konings [24]	-93.286	27.840	$1.23 \cdot 10^{12}$
Mercer and Farrar [21]	-91.136	27.199	$6.49 \cdot 10^{11}$
Nikol'ski [23] RuO steam$_4$ (g)	-90.536	27.020	$5.43 \cdot 10^{11}$
Nikol'ski [23] steam O_2 (g)	15.164	-4.526	$1.08 \cdot 10^{-2}$

As a partial conclusion, relatively large differences in the enthalpies of formation cannot be clearly explained although calorimetric determinations and vapor pressure measurements with saturated RuO_4(g) vapor give enthalpies in the same range. Compared to the calorimetric results, the vapor pressure measurements with the only RuO_4(g) performed by Nikol'skii [23] can be used as the best saturation pressure for the pure compound RuO_4(s, or liq) (reference activity = 1), especially in view of the following thermodynamic analysis of RuO_4 behavior in solution. However, the vaporization of complex gaseous oxides - even in a closed vessel - may be delayed (low vaporization kinetics) and therefore the vapor pressures will be underestimated in the experiments due to an evaporation coefficient < 1. Indeed, from the above pressure values mentioned in table 4, the experimental vapor pressures of Nikol'skii [23] should be increased by a factor of ≈ 44 to reach his calorimetric result [20] corresponding to an evaporation coefficient ≈1/44 = 0.027, as a quite plausible value for the vaporization of complex oxides. This value for an evaporation coefficient is less probable if the solid RuO_4(s) is considered as RuO_4 entities bonded by intramolecular forces.

2 Conclusion

In this work values for thermodynamic functions for RuO_4 solid and liquid are summarized in table 5. For the calorimetric determinations of the enthalpy of formation of the RuO_4 (s) oxide, the dissolution of RuO_4(s) in water will probably made the two calorimetric values quoted compatible. They remain far from the enthalpies resulting from the thermodynamic cycles involving the vapor phase when the latter is mainly composed of RuO_4(g) gas on the condensed oxide. The determination of the vapor pressure is in agreement with DFT calculations of the sublimation enthalpy, and for this reason we propose to retain the third law enthalpy obtained from vapor pressure experimental values.

Table 5. Thermodynamic functions retained in this work for RuO_4 (s) and RuO_4(liquid).

Function	Values for RuO_4 (s or liq)
Cp° (RuO_4, s, cubic) / J K^{-1} mol^{-1}	$-53.426 - 0.32993T + \frac{127.66}{T} + 17.071\sqrt{T}$ (10 to 298K)
S° (RuO_4, s, cubic,298K) / J K^{-1} mol^{-1}	132.7
Δ_f H° (RuO_4, s, cubic, 298K) / kJ mol^{-1}	-252.4 ± 5.5
Δ_{sub}H°(298K) / kJ mol^{-1}	53.4 ± 5.5
T fusion / K	298.6 ± 0.1
Δ_{fus} H° / kJ mol^{-1}	13.3 ± 0.9
Cp° (RuO_4, liquid) / J K^{-1} mol^{-1}	91.598

However, the further calculation of vapor pressures with our proposed data is only valid in the presence of freshly prepared RuO_4(s, or liq) oxide discarding the presence of oxygen produced during storage. Indeed, due to the thermodynamic instability of RuO_4(s) compared to RuO_2(s) and O_2(g), RuO_4 (s, or liq) decomposes at room temperature, and may "explode" when the temperature exceeds 200°C, producing RuO_2(s) and O_2(g). The kinetics of this decomposition suggest a low decomposition rate at low temperatures. As the entropy and heat capacity of the RuO_4(s) compound have not been determined experimentally, we recommend a value obtained by ab-initio calculations. Facing the scattered values for enthalpies of formation of RuO_4, ab-initio data are useful to select the more accurate value. Furthermore, when RuO_4 (s, or liq.) is dissolved in a more or less concentrated acidic environment or with added salts, a vaporization of RuO_4(g) will occur. This vaporization is largely dependent on pH, as the activity of dissolved RuO_4(s) may vary considerably. With Ru nitrate salts, there is also some decomposition of the nitrate producing other molecules than RuO_4(g) in the gas phase. When dissolved in CCl_4 (liq.), the activity of dissolved RuO_4 (liq.) is very low, resulting in low volatilization of RuO_4(g). These volatilization phenomena have been observed in the treatment of nuclear effluents by dissolution in aqueous solutions or solvents, as in the distillation process.

3 Acknowledgements

I.N. ,C.C., E.F. thank IRSN (France) for the financial support (contract number IRSN-LS20317). The authors would like to thank Sidi Souvi, Bénédicte Michel and Marc Barrachin for their helpful discussions and comments on this work. This work was made possible by the HPC resources of the CCGT/CCRT.

4 Appendix

Appendix A: Thermodynamic data for low temperature solid RuO_4

Computational method

All calculations are performed in the DFT framework as implemented in the Quantum Espresso package [38]. The Perdew-Burke-Ernzerhof [39] function constructed in the generalized gradient approximation (GGA) is used to calculate the exchange and correlation energies. Ultra-soft pseudopotentials are used to model the ionic nuclei while only valence electrons are explicitly considered (semi-core electrons are included in the pseudopotentials). To ensure the cohesion of the crystal, especially during the lattice optimization step, Van der Waals corrections are necessary as ruthenium tetroxide exhibits a molecular crystal behavior. In this work, long-range interactions are taken into account using the DFT-D [40]. The convergence threshold on forces has been set at 7.2×10^{-4} eV/Å whereas the default value is considered on energy. In addition, the criterion for the residual pressure during the cell optimization is set at 0.05 kbar. The Brillouin zone (BZ) sampling and plane wave cut-off energy were adjusted to satisfy a convergence criterion of 2 meV/f.u on electronic energy. The BZ grids were extended to 2 × 2 × 2 and 2 × 3 × 2 for cubic and monoclinic crystal stacks, respectively. The plane wave cut-off energy is fixed at 1142 eV for both cells. The vibrational properties of ruthenium tetroxide are calculated from phonon data computed with the finite displacement method as implemented in the Phonopy [41] tool. The sizes of primitive cells are large enough to accurately calculate the phonons at Γ for the cubic cell while a 1 × 2 × 1 supercell is used for the monoclinic cell. Two different arrangements are studied, a cubic and a monoclinic crystal structure. The cubic unit cell is described by an arrangement of 8 RuO_4 patterns while only 4 units describe the monoclinic crystal structure (see Ref. [42] for more details on crystallographic data as well as the initial atomic coordinates).

In a complementary way, the RuO_4 molecule is also briefly studied with a similar approach to obtain the sublimation enthalpy. In this case, the calculation is performed in a 15 Å cubic cell and the plane wave cut-off energy is set to 1224 eV.

Results

Comparison of the total energies of the two crystal structures shows that the cubic structure is the more stable at 0 K, although the energy difference is extremely small (0.18 kJ/mol f.u. or 1.9 meV/f.u., including ZPE). Taking into account the effect of temperature in the harmonic approximation, the Helmotz vibrational energies remain degenerate up to room temperature. Therefore, the phase stability cannot be definitively stated and the present results tend to confirm the crystal polymorphism of ruthenium tetroxide in accordance with the most recent experimental study [42].

Thermodynamic properties such as standard entropy (S^{θ} (T)), heat capacity, enthalpy increment (H(T) - H(0)) and Gibbs energy function can be calculated from the vibrational data.

The first properties are mandatory for a critical evaluation of the experimental calorimetric results, in particular the Gibbs energy function Φ(T), of each species concerned. This property is expressed as follows:

$$\Phi(T) = S^{\theta}(T) - \frac{H(T)-H(0)}{T} \quad \text{(A.1)}$$

The obtained data are fitted with the following function:

$$\Phi(T) = a_1 + a_2 \times T + a_3 \times \ln(T) + \frac{a_4}{T} + \frac{a_5}{\sqrt{T}} \quad \text{(A.2)}$$

where T is given in Kelvin. The heat capacity can be expressed as:

$$C_{V/P}(T) = b_1 + b_2 \times T + \frac{b_3}{T} + b_4 \times \sqrt{T} \qquad \text{(A.3)}$$

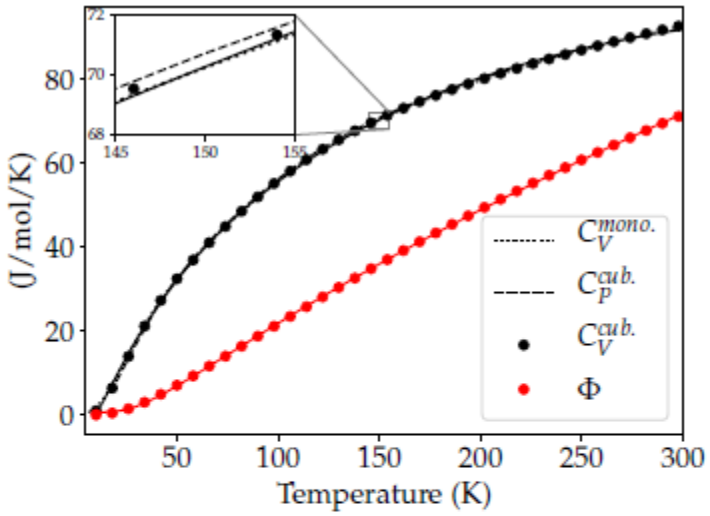

*Figure A-1. Comparison of calculated heat capacity at both constant volume (harmonic) and constant pressure(quasi-harmonic) for the cubic crystal (**cub**.) as well as heat capacity at constant volume for the monoclinic one (**mono**). Calculated Gibbs energy function (Φ) is computed for the cubic crystal of ruthenium tetraoxide whitin harmonic approach. Straight lines correspond to the interpolation with Equation 1 and 2 of computed data (dashed lines and dots).*

The quasi-harmonic calculation showed no deviation from the harmonic approximation in the interval 0 K to room temperature interval (highlighted by the heat capacity property, see figure A-1), so it can be assumed in this case that the harmonic approximation gives an acceptable evaluation of the vibration data.
The parameters obtained for the two functions are summarized in Table A-1.

Table A-1. Parameters of the Gibbs energy function (Eq. 1) and the heat capacity (Eq.2) for the cubic crystal of ruthenium tetraoxide. Parameters lead to properties given in J/mol/K.

	$\Phi(T)$		$C_{V/P}(T)$
a_1	-3.4033×10^2	b_1	-5.3426×10^1
a_2	1.0503×10^{-1}	b_2	-3.2993×10^{-1}
a_3	5.7478×10^1	b_3	1.2766×10^2
a_4	-9.9755×10^2	b_4	1.4071×10^1
a_5	9.6980×10^2	-	-

These sets of thermodynamic functions complete the missing thermodynamic data needed to interpreting calorimetric experiments.
The difference in enthalpy between the gas and the solid, the sublimation enthalpy, is calculated using the properties of the solid and the gas according to the formula:

$$\Delta_{sub}H^o_{298} = E_{elec}\left(RuO_{4(g)}\right) - E_{elec}\left(RuO_{4\,(s)}\right) + \Delta ZPE + \Delta(H_{298} - H_0)$$

where E_{elec} is the electronic energy at 0 K whereas ΔZPE and $\Delta(H_{298}-H_0)$ correspond to the difference between gaseous and solid phase of the zero-point energy and enthalpy increment, respectively.

Table A-2. Entropy, enthalpy of sublimation and enthalpy of formation of RuO_4 compound calculated within harmonic approximation for the cubic crystal structure compared to published ones in thermodynamic databases. Theoretical values from Material Project [43] and OQMD [44] and databases are computed at 0K and do not includes the zero point energy whereas all other values are calculated at 298.15K. Our uncertainty on $\Delta_f H^\theta$ corresponds to the one of heat of formation of RuO_4 (g) evaluated in Ref. [15].

Reference	Δ_f H°$_{298}$ RuO_4(s) / kJ mol^{-1}	$\Delta_{sublim.}$ H°$_{298}$ RuO_4(s) / kJ mol^{-1}	S°$_{298}$ RuO_4(s) / J K^{-1} mol^{-1}
OQMD database [44]	-418	-	-
MP database [43]	-576	-	-
Cordfunke et al [24]	-243 ± 7	54.8 ± 2.4	137.3 ± 8
Online database [26]	-239.3 ± 5.4	55.2 ± 0.8	141
This DFT work	-251.0 ± 5.5	53.4	132.7

The computed sublimation enthalpy (Table A-2) is close to published values in accordance to evaluated uncertainty of Ref. [24]. From sublimation enthalpy, the standard heat of formation of crystal can be deduced by:

$$\Delta_f H^o_{298}(RuO_{4(s)}) = \Delta_f H^o_{298}(RuO_{4(g)}) - \Delta_{sub} H^o_{298}(RuO_{4(s)})$$

relation where the standard heat of formation of RuO_4(g) is taken from recent critical assessment (-197.6±5.5 kJ/mol [15]). Usually, the standard heat of formation is computed from elements under their most stable states: $Ru_{(c)}$, $O_{2(g)}$ for ruthenium tetroxide. Unfortunately, this approach is excluded in the present work because the overbinding of GGA functional in the O_2 molecule as expected [45] would approximately induce an error of about 200 kJ/mol on the standard heat of formation.
Furthermore, this calculation scheme would involve species having too different chemical binding leading to an additional bias. These statements could explain the huge gap between our value and those coming from DFT databases [43, 44], the fact that their DFT methodologies do not include long range interactions additionally induces differences. Finally, present approach tends to get the most accurate theoretical heat of formation: $\Delta_f H^\theta$ = -251.0 ± 5.5 kJ/mol.

Appendix B. Estimated entropy via Latimer's rule

In the absence of experimental data on the specific heat at low temperature $C°_p$, another conventional method was used to estimate the entropy. Moreover, it was used as a cross check for ab initio calculations as well as an indication of the general uncertainty for the entropy.
The estimate can be done from the Latimer 's rule [27-29] based on ionic contributions to entropy at 298 K for oxides and compounds. In Table B-**Erreur ! Source du renvoi introuvable.**1 we mention the calculations with Latimer's rule at beginning for RuO_2(s), whose experimental value is known and can be used for scaling, and, then, an evaluation is made for the RuO_4(s) from the Latimer contribution for O^{2-} with a cation of degree +8. For the later degree, in figure B-1 two types of smoothing are used to obtain the contribution of each oxygen for a +8 charge of the Ru cation.

Table B-1. Latimer rule estimation and comparison with selected experimental data.

Origine	$S°_{298}$ Ru	$S°_{298}$ O^{2-}	$S°_{298}$ $RuO_2(s)$	$S°_{298}$ $RuO_4(s)$
Latimer table[27, 28]	53	3.2	59.4	140.7
Experimental Ru[20] + Latimer for O^{2-}	28.614	3.2	35.014	116.3
Re-calculated	**28.614**	8.768*	**46.15**	132.5**

** calculated contribution O^{2-} from experimental $RuO_2(s)$ entropy value;*

*** calculated from the average of the two extrapolations in Figure B-1.*

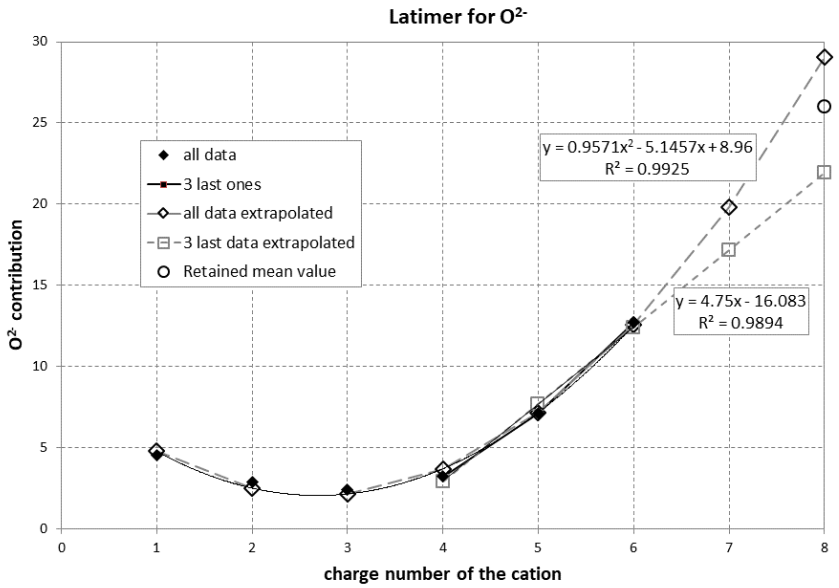

Figure B-1. Application of Latimer's rule to estimate the contribution of the O^{2-} ion in a compound with several oxidation states.

The application of the original Latimer's rule for $RuO_2(s)$ shows that this rule largely underestimates the contribution of oxygen (3.2 instead of 8.8 deduced from reliable experimental RuO_2 entropy value). Thus, the Latimer's value applied to $RuO_4(s)$ entropy could be underestimated as presented in the second raw. Correction based on known $RuO_2(s)$ produces an entropy that agrees with the DFT value.

5 References

[1] R. Thoma, Phase diagrams of nuclear reactor materials, Oak Ridge National Lab., Tenn., ORNL-2548, W-7405-ENG-26,(1959), https://doi.org/10.2172/4234144.

[2] F. Garisto, Thermodynamic behaviour of ruthenium at high temperatures, Atomic Energy of Canada Ltd., Pinawa, MB (Canada). , AECL-9552, (1988), https://inis.iaea.org/search/search.aspx?orig_q=RN:22068402.
[3] K. Motojima, Removal of Ruthenium from PUREX Process, Journal of Nuclear Science and Technology, 26 (1989) 358-364, https://doi.org/10.1080/18811248.1989.9734317.
[4] B. Eichler, F. Zude, W. Fan, N. Trautmann, G. Herrmann, Volatilization and deposition of ruthenium oxides in a temperature gradient tube, Radiochimca Acta, 56 (1992) 133-140, https://doi.org/10.1524/ract.1992.56.3.133.
[5] C. Mun, L. Cantrel, C. Madic, Review of Literature on Ruthenium Behavior in Nuclear Power Plant Severe Accidents, Nuclear Technology, 156 (2006) 332-346, https://doi.org/10.13182/NT156-332.
[6] A. Auvinen, G. Brillant, N. Davidovich, R. Dickson, G. Ducros, Y. Dutheillet, P. Giordano, M. Kunstar, T. Kärkelä, M. Mladin, Y. Pontillon, C. Séropian, N. Vér, Progress on ruthenium release and transport under air ingress conditions, Nuclear Engineering and Design, 238 (2008) 3418-3428, https://doi.org/10.1016/j.nucengdes.2008.07.010.
[7] J. Holm, H. Glänneskog, C. Ekberg, Interactions of RuO4 (g) with different surfaces in nuclear reactor containments, Technical report, NKS, Nordisk kernesikkerhedsforskning, 8778932319, (2008), https://inis.iaea.org/search/search.aspx?orig_q=RN:39104583.
[8] J. Holm, H. Glänneskog, C. Ekberg, Deposition of RuO4 on various surfaces in a nuclear reactor containment, Journal of Nuclear Materials, 392 (2009) 55-62, https://doi.org/10.1016/j.jnucmat.2009.03.047.
[9] E. Beuzet, J.-S. Lamy, H. Perron, E. Simoni, G. Ducros, Ruthenium release modelling in air and steam atmospheres under severe accident conditions using the MAAP4 code, Nuclear Engineering and Design, 42 (2012) 157-162, https://inis.iaea.org/search/search.aspx?orig_q=RN:42044303.
[10] P. Swain, C. Mallika, R. Srinivasan, U.K. Mudali, R. Natarajan, Separation and recovery of ruthenium: a review, J Radioanal Nucl Chem, 298 (2013) 781-796, https://doi.org/10.1007/s10967-013-2536-5.
[11] T. Kato, T. Usami, T. Tsukada, Y. Shibata, T. Kodama, Study on volatilization mechanism of ruthenium tetroxide from nitrosyl ruthenium nitrate by using mass spectrometer, Journal of Nuclear Materials, 479 (2016) 123-129, https://doi.org/10.1016/j.jnucmat.2016.06.052.
[12] C. Lefebvre, T. Dumas, C. Tamain, T. Ducres, P.L. Solari, M.-C. Charbonnel, Addressing Ruthenium speciation in tri-n-butyl-phosphate solvent extraction process by Fourier transform infrared, extended X-ray absorption fine structure, and single crystal X-ray diffraction, Industrial & Engineering Chemistry Research, 56 (2017) 11292-11301, https://doi.org/10.1021/acs.iecr.7b02973.
[13] I. Kajan, H. Lasseson, I. Persson, C. Ekberg, Interaction of ruthenium tetroxide with surfaces of nuclear reactor containment building, Journal of Nuclear Science and Technology, 53 (2016) 1397-1408, https://doi.org/10.1080/00223131.2015.1120245.
[14] C. Chatillon, I. Nuta, F.-Z. Roki, E. Fischer, Chemical thermodynamics of RuO2(s), Journal of Nuclear Materials, 509 (2018) 742-751, https://doi.org/10.1016/j.jnucmat.2018.05.060.
[15] I. Nuta, C. Chatillon, F.-Z. Roki, E. Fischer, Gaseous phase above Ru–O system: A thermodynamic data assessment, Calphad, 75 (2021) 102329, https://doi.org/10.1016/j.calphad.2021.102329.
[16] SGPS(SGPSBase.tdb), SGTE Pure substances database (v13.1, revised 2019) in Factsage 8.0 software

[17] F. Miradji, S. Souvi, L. Cantrel, F. Louis, V. Vallet, Thermodynamic Properties of Gaseous Ruthenium Species, The Journal of Physical Chemistry A, 119 (2015) 4961-4971, https://doi.org/10.1021/acs.jpca.5b01645.
[18] H. Debray, H. Joly, Recherches sur le Ruthénium: acide hypzerruthènique, Compt. Rend. Acad. Sci. Paris, 106 (1888) 328-333,
[19] A.B. Nikol'skii, Existence of two modifications of Ruthenium tetroxide, Russ. J. Inorg. Chem., 8 (1963) 668-669,
[20] A.B. Nikol'skii, A.N. Ryabov, Determination of the Heat of Formation of Ruthenium Tetroxide, Russ. J. Inorg. Chem. (Engl. Transl.), 9 (1964) 3-5,
[21] E.E. Mercer, D.T. Farrar, Heats of Formation of RuO4 and RuO_4^{2-} and Related Compounds, Can. J. Chem., 47 (1969) 581-586, https://doi.org/10.1139/v69-089.
[22] Y. Koda, Boiling points and ideal solutions of ruthenium and osmium tetraoxides, Journal of the Chemical Society, Chemical Communications, (1986) 1347-1348, https://doi.org/10.1039/C39860001347.
[23] A.B. Nikol'skii, Saturated Vapour Pressure of Ruthenium Tetroxide, Russ. J. Inorg. Chem. (Engl. Transl.), 8 (1963) 541-543, https://www.osti.gov/biblio/4666430.
[24] E.H.P. Cordfunke, R.J.M. Konings, Thermochemical data for reactor materials and fission products, North-Holland, Elsevier Science Publishers, Amsterdam, ISBN 0-444-88-485-8, 1990, pp.
[25] V. Piccialli, Ruthenium tetroxide and perruthenate chemistry. Recent advances and related transformations mediated by other transition metal oxo-species, Molecules, 19 (2014) 6534-6582, https://doi.org/10.3390/molecules19056534.
[26] C. NET, http://www.chem.msu.ru/cgi-bin/tkv.pl., Departement of Chemistry of Moscow State University, (1994).
[27] O. Kubaschewski, C.B. Alcock, P.J. Spencer, Materials Thermochemistry, by 6th ed., Pergamon Press, 1993, pp.172-174.
[28] W.M. Latimer, Methods of Estimating the Entropies of Solid Compounds, Journal of the American Chemical Society, 73 (1951) 1480-1482, https://doi.org/10.1021/ja01148a021.
[29] W.M. Latimer, W.H. Rodebush, Polarity and ionization from the standpoint of the lewis theory of valence, Journal of the American Chemical Society, 42 (1920) 1419-1433, https://doi.org/10.1021/ja01452a015.
[30] M.W. Chase, NIST-JANAF Thermochemical Tables, J. Phys. Chem. Ref. Data Monograph 9 (1998),
[31] I. Prigogine, R. Defay, Thermodynamique Chimique, Dunod, Paris, 1950, pp.19-31.
[32] G.W. Watt, W.C. McMordie, The Interaction of ruthenium tetroxide and ammonia, J. Inorg. Nucl. Chem., 27 (1965) 262-263, https://doi.org/10.1016/0022-1902(65)80225-1.
[33] J.G. Dillard, R.W. Kiser, Ionization and Dissociation of Ruthenium and Osmium Tetroxides1, The Journal of Physical Chemistry, 69 (1965) 3893-3897, https://doi.org/10.1021/j100895a042.
[34] R.D. Brittain, D.L. Hildenbrand, Gas phase reaction of Ruthenium Tetroxide with Nitrogen Oxides, SRI International, DOE/SR/00001- - Tl20, (1985) 22, https://www.osti.gov/biblio/6954085.
[35] M.H. Ortner, C.J. Anderson, P.F. Campbell, Research and development studies on waste storage process, Vitro Laboratories, report IDO-14504, (1961) 133, https://www.osti.gov/biblio/4834683.
[36] M. Ortner, Infrared spectrum and thermodynamic properties of ruthenium tetroxide, The Journal of Chemical Physics, 34 (1961) 556-558, https://doi.org/10.1063/1.1700982.
[37] C. Mun, L. Cantrel, C. Madic, Study of RuO 4 decomposition in dry and moist air, Radiochimica Acta - RADIOCHIM ACTA, 95 (2007) 643-656, https://doi.org/10.1524/ract.2007.95.11.643.

[38] P. Giannozzi, S. Baroni, N. Bonini, M. Calandra, R. Car, C. Cavazzoni, D. Ceresoli, G.L. Chiarotti, M. Cococcioni, I. Dabo, A. Dal Corso, S. de Gironcoli, S. Fabris, G. Fratesi, R. Gebauer, U. Gerstmann, C. Gougoussis, A. Kokalj, M. Lazzeri, L. Martin-Samos, N. Marzari, F. Mauri, R. Mazzarello, S. Paolini, A. Pasquarello, L. Paulatto, C. Sbraccia, S. Scandolo, G. Sclauzero, A.P. Seitsonen, A. Smogunov, P. Umari, R.M. Wentzcovitch, QUANTUM ESPRESSO: a modular and open-source software project for quantum simulations of materials, Journal of Physics: Condensed Matter, 21 (2009) 395502, https://doi.org/10.1088/0953-8984/21/39/395502.
[39] J.P. Perdew, K. Burke, M. Ernzerhof, Generalized Gradient Approximation Made Simple, Physical Review Letters, 77 (1996) 3865-3868, https://doi.org/10.1103/PhysRevLett.77.3865.
[40] V. Barone, M. Casarin, D. Forrer, M. Pavone, M. Sambi, A. Vittadini, Role and effective treatment of dispersive forces in materials: Polyethylene and graphite crystals as test cases, Journal of computational chemistry, 30 (2009) 934-939, https://doi.org/10.1002/jcc.21112.
[41] A. Togo, I. Tanaka, First principles phonon calculations in materials science, Scripta Materialia, 108 (2015) 1-5, https://doi.org/10.1016/j.scriptamat.2015.07.021.
[42] M. Pley, M.S. Wickleder, Two crystalline modifications of RuO4, Journal of Solid State Chemistry, 178 (2005) 3206-3209, http://dx.doi.org/10.1016/j.jssc.2005.07.021.
[43] A. Jain, S.P. Ong, G. Hautier, W. Chen, W.D. Richards, S. Dacek, S. Cholia, D. Gunter, D. Skinner, G. Ceder, K.A. Persson, Commentary: The Materials Project: A materials genome approach to accelerating materials innovation, APL Materials, 1 (2013) 011002, https://doi.org/10.1063/1.4812323.
[44] S. Kirklin, J.E. Saal, B. Meredig, A. Thompson, J.W. Doak, M. Aykol, S. Rühl, C. Wolverton, The Open Quantum Materials Database (OQMD): assessing the accuracy of DFT formation energies, npj Computational Materials, 1 (2015) 15010, https://doi.org/10.1038/npjcompumats.2015.10.
[45] L. Wang, T. Maxisch, G. Ceder, Oxidation energies of transition metal oxides within the GGA+U framework, Physical Review B, 73 (2006) 195107, https://doi.org/10.1103/PhysRevB.73.195107.